Histopathology 2010, **56**, 510–522. DOI: 10.1111/j.1365-2559.2010.03512.x

Microvascular irregularities are associated with composition of squamous epithelial lesions and correlate with subepithelial invasion of superficial-type pharyngeal squamous cell carcinoma

Satoshi Fujii, Manabu Yamazaki, Manabu Muto[1] & Atsushi Ochiai

Pathology Division, Research Centre for Innovative Oncology, National Cancer Centre at Kashiwa, Chiba, and [1]Department of Gastroenterology and Hepatology, Kyoto University Graduate School of Medicine, Kyoto, Japan

Date of submission 30 April 2009
Accepted for publication 25 July 2009

Fujii S, Yamazaki M, Muto M & Ochiai A
(2010) *Histopathology* **56**, 510–522

Microvascular irregularities are associated with composition of squamous epithelial lesions and correlate with subepithelial invasion of superficial-type pharyngeal squamous cell carcinoma

Aims: Superficial squamous epithelial lesions of the pharynx are increasingly recognized by architectural changes in the intraepithelial papillary capillary loop (IPCL) assessed by narrow-band imaging (NBI). The aim was to explore the histology of squamous epithelial precursor lesions and superficial-type pharyngeal squamous cell carcinoma (STPSCC), including squamous cell carcinoma (SCC) *in situ* and early invasive SCC, by focusing on microvascular irregularities to investigate the composition of those lesions and to explore the pathological characteristics of STPSCCs.

Methods and results: Several pathological factors including thickness of intraepithelial squamous cell carcinoma (IESCC) and tumour thickness and microvascular density (MVD) were examined in 104 STPSCCs from 69 patients. The results show that architectural change of IPCL was recognized in precursor lesions in parallel with architectural disturbance and cytological atypia for criteria of diagnosing dysplasia. In 104 STPSCCs, the MVD of IESCC was correlated with the thickness of IESCC ($P = 0.0115$). Moreover, invasive SCC showed significantly higher MVD of IESCC ($P = 0.0078$) and there was significant correlation between the thickness of IESCC and subepithelial invasion ($P < 0.0001$).

Conclusions: Microvascular irregularities are an important pathological factor in carcinogenesis and early invasiveness of SCC of the pharynx.

Keywords: intraepithelial papillary capillary loop, microvascular density, microvascular irregularities, narrow-band imaging, superficial-type pharyngeal squamous cell carcinoma

Abbreviations: EMR, endoscopic mucosal resection; ESCC, oesophageal squamous cell carcinoma; ESD, endoscopic submucosal dissection; H&E, haematoxylin and eosin; IESCC, intraepithelial squamous cell carcinoma; IPCL, intraepithelial papillary capillary loop; mLVL, multiple Lugol-voiding lesion; MVD, microvascular density; NBI, narrow-band imaging; SCC, squamous cell carcinoma; STPSCC, superficial-type pharyngeal squamous cell carcinoma; UADT, upper aerodigestive tract

Introduction

In Japan, the estimated number of new cancer cases of the mouth/pharynx per 1000 is <5.0 and the estimated age-standardized rates of cancer incidence of the mouth/pharynx per 100 000 is <5.0.[1] Formerly, clinicians had difficulty in detecting pharyngeal cancer until it had progressed to the advanced stage.

Address for correspondence: A Ochiai, Pathology Division, Research Centre for Innovative Oncology, National Cancer Centre at Kashiwa, 651 Kashiwanoha, Kashiwa, Chiba 277 8577, Japan. e-mail: aochiai@east.ncc.go.jp

Therefore, it was necessary to detect pharyngeal cancer at an early stage to avoid extensive surgical resection, causing a loss of function with respect to swallowing and/or speaking, and cosmetic deformities. Recently, the advent of narrow-band imaging (NBI) endoscopy with magnification has dramatically improved the detection of squamous precursor lesions and early-stage SCC of the pharynx.[2] NBI is a novel optical technique that uses reflected light to visualize the superficial structure of an organ surface.[3] It has previously been reported that the morphological changes in microvascular structure are useful in the diagnosis of superficial oesophageal carcinomas.[4,5] NBI utilizes the structural change of microvessels referred to as the intraepithelial papillary capillary loop (IPCL) in mucosal lesions of early-stage SCC of the pharynx.[2] This microvascular structural change is enhanced by NBI and an image allowing a conclusive diagnosis can be obtained.

Most pharyngeal cancer is SCC. It has been accepted that dysplasia may progress to SCC *in situ* and eventually to invasive SCC. The pathological assessment of precursor lesions in oropharynx and hypopharynx is similar throughout the upper aerodigestive tract (UADT).[6] Precursor lesions have been grouped under the term dysplasia (mild, moderate

Table 1. Patient population treated with EMR/ESD

Gender	
Male	67 (97.1%)
Female	2 (2.9%)
Age	
Median/mean (range)	62/62.2 (42–88)
mLVLs	
Presence	60 (87.0%)
None	7 (10.1%)
Unknown	2 (2.9%)
Multiple STPSCC	
Presence	30 (43.5%)
None	39 (56.5%)
Overlapping ESCC	
Presence	62 (89.9%)
None	7 (10.1%)
Multiple HNSCC	
Presence	24 (34.8%)
None	45 (65.2%)

mLVLs, multiple Lugol-voiding-lesions; STPSCC, superficial type pharyngeal squamous cell carcinoma; ESCC, oesophageal squamous cell carcinoma; HNSCC, head & neck squamous cell carcinoma.

Table 2. Clinicopathological factors of 104 STPSCCs treated with EMR/ESD

Primary site	
Oropharynx	13 (12.5%)
Upper wall	2 (1.92%)
Anterior wall	2 (1.92%)
Posterior wall	4 (3.85%)
Lateral wall	5 (4.81%)
Hypopharynx	91 (87.5%)
Pyriform sinus	75 (72.1%)
Postcricoid	6 (5.8%)
Posterior wall	6 (5.8%)
Arytenoid	4 (3.8%)
Tumour size (mm)	
≤5	20 (19.2%)
5< and ≤10	40 (38.5%)
10< and ≤20	31 (29.8%)
20< and ≤30	10 (9.6%)
30< and ≤40	3 (2.9%)
Subepithelial invasion	
Presence	29 (27.9%)
None	75 (72.1%)
Vessel infiltration	
Presence	6 (5.8%)
None	98 (94.2%)
Lymph node metastasis*	
Presence	1 (0.96%)
None	103 (99.04%)
Local recurrence	
Presence	3 (2.9%)
None	101 (97.1%)

*Metachronous lymph node metastasis.

and severe dysplasia). In order to make a precise pathological diagnosis of squamous epithelial lesions detected by NBI endoscopy, it is necessary to understand the pathological findings by focusing on the irregularities of the microvasculature, i.e., IPCL. Detecting pharyngeal SCC *in situ* would clearly be of benefit to patients. It is also necessary to detect those pathological features that reflect the potential for subepithelial invasion and metastasis to lymph nodes, thus leading to selecting optimal therapy for early-stage SCC.

There is a specific characteristic of the pharynx, i.e. it has no lamina muscularis mucosae; this implies that evaluations such as 'invasion of the lamina propria mucosae' or 'invasion of the submucosal layer', as in oesophageal cancer specimens, are impossible in the pharynx. The invasive depth of oesophageal SCC correlates with risk factors such as vessel infiltration and lymph node metastasis.[7] Thus, it is essential to identify critical risk factors such as these in early-stage SCC. In organs such as the tongue, which has no lamina muscularis mucosae, tumour thickness has been reported to be a risk factor for cervical lymph node metastasis.[8,9] In our institution, SCC *in situ* of the oropharynx and hypopharynx have previously been detected using the NBI system.[10] We have now accumulated >100 patients with superficial-type pharyngeal squamous cell carcinoma (STPSCC) resected by endoscopic resection [endoscopic mucosal resection (EMR) or endoscopic submucosal dissection (ESD)] who have an extended clinical follow-up period to enable us to investigate the clinicopathological features and clinical course of STPSCC.

Materials and methods

PATIENT POPULATION

One hundred and four lesions from 69 patients (67 male and two female, median age 62 years) were consecutively collected for the present study. These patients underwent EMR or ESD between June 2002 and September 2006 at the National Cancer Centre

Table 3. Histological findings of squamous epithelial lesions of the pharynx based on microvascular irregularities

	Normal	Inflammation	Mild dysplasia	Severe dysplasia	SCC-*in-situ*	Invasive SCC
IPCL extension upward	(–)	Mid zone	Superficial zone	Superficial zone	Superficial zone	Superficial zone
IPCL dilatation and branching	(–)	(–) ~ Slight	(+)	(+)	(+)	(+); Complicated
IPCL diameter expansion	(–)	(–)	Mild ~ severe	Severe	Severe	Severe
Proliferative cell distribution	AB	(–)	LI ~ LH	S	S	D
Basal cell palisading	(+)	(+/–), Edematous	(+)	(+)	(+/–)	–
Basal cell enlargement	(–)	(–)	(–)	(+/–)	(+)	(+)
Spinous laryer retention	(+)	(+)	(+)	(–)	(–)	(–)
Superficial layer retention	(+)	(+)	(+)	(+)	(–)	(–)
Nuclear arrangement	PP	PP	PP	PL	PL	PL
Nuclear density	NI	NI	IM	IS	IS	IS
Subepithelial solitary cell nest	(–)	(–)	(–)	(–)	(–)	(+)

SCC, squamous cell carcinoma; IPCL, intra-epithelial papillary capillary loop; Proliferative cell, cells labelled immunohistochemically by MIB-1 AB, arranged in the basal layer; LI, localized at the peri-IPCL; LH, limited to the lower third of intra-epithelial layer; S, scattered in intra-epithelial layer; D, distributed densely in the intra-epithelial layer; PP, polarity preserved; PL, polarity lost; NI, not increased; IM, increased mildly at the peri-IPCL or the lower third of intra-epithelial layer; IS, increased severely throughout the intra-epithelial layer.

Hospital East. Pre-operative examinations identified no metastasis, including lymph node metastasis, in any of the patients, and none had received prior anticancer treatment. These 69 cases are summarized in Table 1. Eighty-seven percent of patients in the current study had multiple Lugol-voiding lesions (mLVLs) in the background oesophageal mucosa. The presence of mLVLs in background oesophageal mucosa was evaluated by Lugol's iodine staining clinically. Multiple STPSCCs at oropharyngeal and hypopharyngeal mucosal sites were identified in 30 patients (43.5%). Furthermore, 62 patients (89.9%) had overlapping oesophageal SCC, and 24 (34.8%) had multiple head and neck SCCs apart from STPSCC. Multiple STPSCC or overlapping oesophageal squamous cell carcinoma (ESCC) or multiple head and neck squamous cell carcinoma were managed until the end of the follow-up period.

All informed consent processes were conducted in accordance with the guidelines of the National Cancer Centre Hospital East institutional review board authorization for this study.

CLINICOPATHOLOGICAL FACTORS OF STPSCCS TREATED WITH EMR/ESD

One hundred and four consecutive STPSCCs were detected by conventional endoscopy and NBI endoscopy with magnification and a pathological diagnosis of SCC was made by biopsy specimen before EMR/ESD. The clinicopathological factors of the 104 STPSCCs treated with EMR/ESD are summarized in Table 2. The pyriform sinus was the most common primary site (72.1%). Tumour diameters ranged from 1.3 to 40 mm and median and average tumour diameters were 10 and 12.23 mm, respectively.

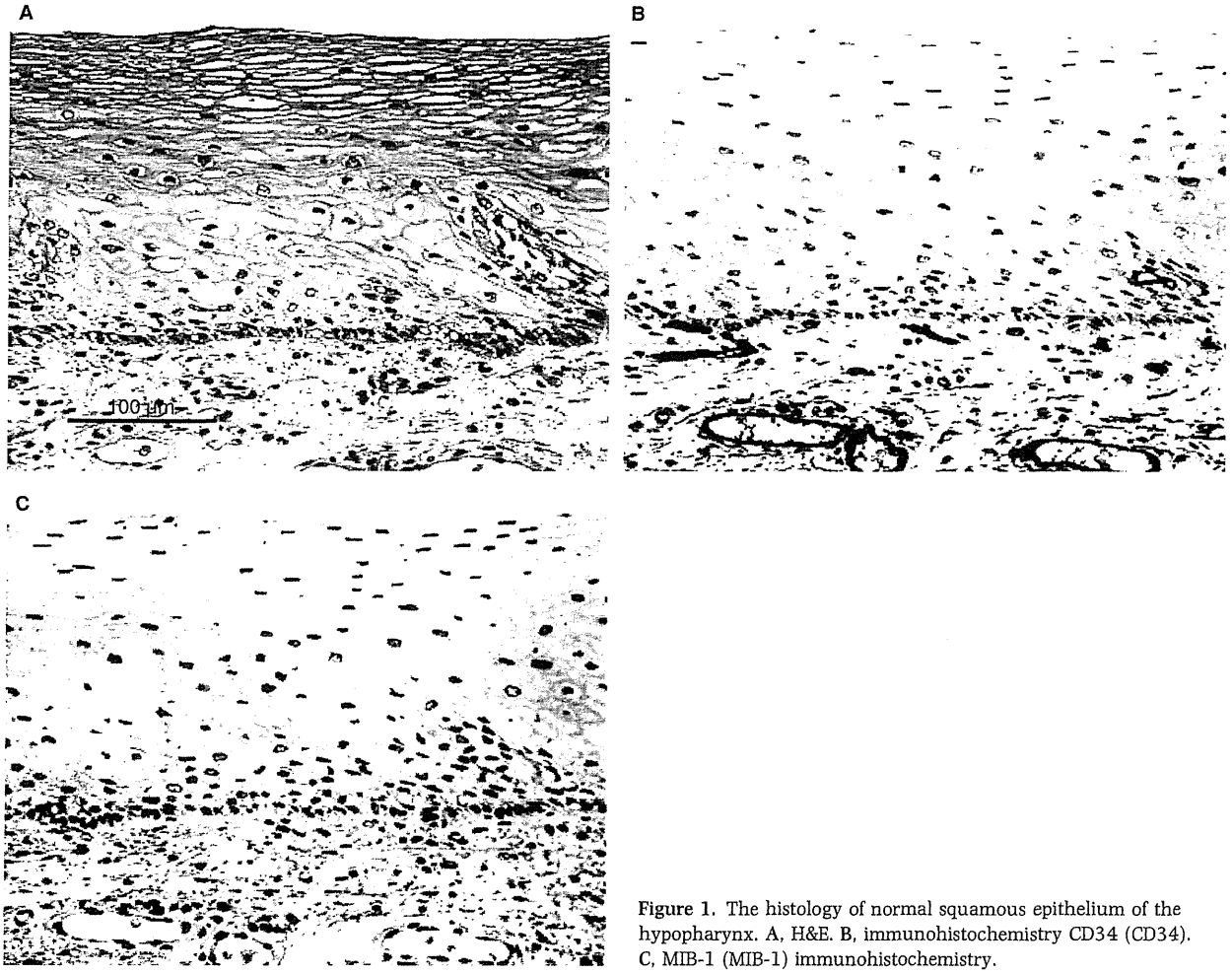

Figure 1. The histology of normal squamous epithelium of the hypopharynx. A, H&E. B, immunohistochemistry CD34 (CD34). C, MIB-1 (MIB-1) immunohistochemistry.

Tumour size was measured after mapping of the SCC tissue by histological evaluation. Twenty-nine lesions (27.9%) were pathologically confirmed to be invasive SCC. Subepithelial invasion was defined as at least one solitary carcinoma cell nest being observed in the subepithelial region. Only six lesions (5.8%) showed blood vessel infiltration identified by elastic staining and only one case (0.96 %) showed lymphatic vessel infiltration by haematoxylin and eosin (H&E) staining. Vessel infiltration included lymphatic and/or blood vessel infiltration. Only one (0.96%) had metachronous lymph node metastasis and only three STPSCCs recurred locally. The average follow-up period was 826 days (median 726 days, SD 464.6 days).

INDICATIONS FOR BIOPSY

Biopsy specimens collected by endoscopists on suspicion of or to rule out SCC were also used to examine diagnostic histological findings on the basis of microvascular irregularities in non-neoplastic lesions, dysplasia, SCC *in situ* and invasive SCC together with magnified NBI images.

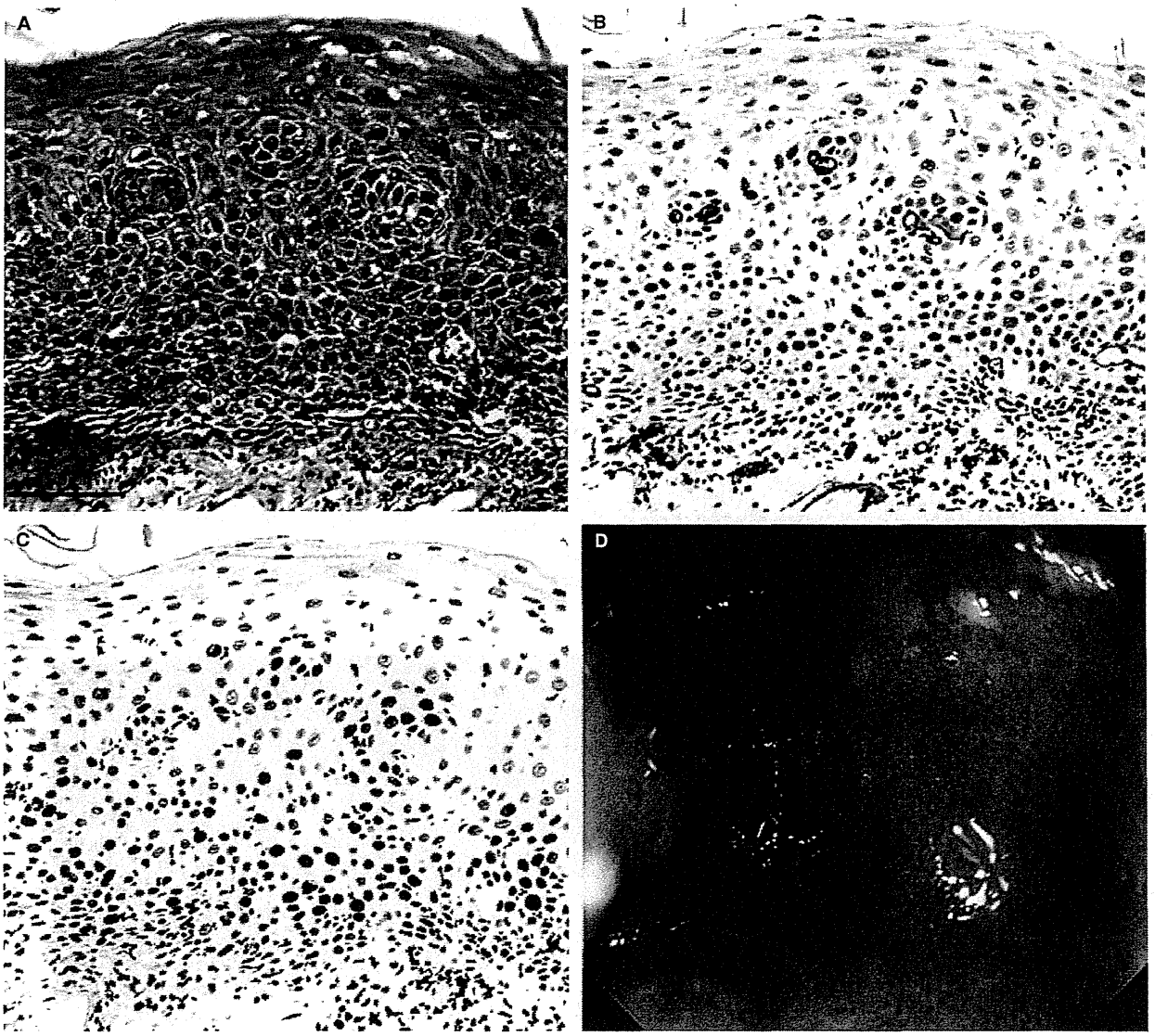

Figure 2. The histology of an inflammatory lesion from a biopsy specimen. A, H&E. B, CD34. C, MIB-1. D, Narrow-band imaging (NBI) endoscopy with magnification of the hypopharynx (right arytenoid).

HISTOLOGICAL METHODS

All specimens resected by EMR/ESD were fixed in 10% formalin and embedded in paraffin wax. The tissue specimens were cut at a thickness of 2 μm and all sections were routinely evaluated for pathological diagnosis. The pathological parameters for each case were then profiled and used for further analyses. The section with the thickest tumour diameter measured from the tumour surface to the base of the malignant tissue was selected for further immunohistochemical analysis, and serial 4-μm thick sections were used for immunohistochemistry to detect IPCL and calculate microvascular density (MVD). To calculate the MVD, blood vessels were displayed using anti-CD34 antibody (Dako, Carpinteria, CA, USA) (dilution 1:50) on 4 μm thick sections. Antigen retrieval was carried out using microwave treatment in citrate buffer (pH 6.0). Sections were processed immunohistochemically using the Dako Envision system. Diaminobenzidine was used as the chromogen and haematoxylin as the counterstain.

CRITERIA FOR PATHOLOGICAL DIAGNOSIS

For the diagnosis of dysplasia and SCC *in situ* and invasive SCC, the criteria proposed by the World Health Organization were used.[6] These criteria are used for diagnosing dysplasia, based on architectural and cytological abnormalities. However, endoscopists have recently discovered early-stage lesions in pharynx using the NBI system. NBI utilizes change in the IPCL in squamous epithelium. That is, the change in IPCL should be accompanied by the architectural and cytological criteria for diagnosing dysplasia. Therefore, the morphological changes seen as microvascular irregularities in intraepithelial lesions should be considered in the pathological diagnosis together with architectural and cytological abnormalities.

In UADT, the general guideline for measuring the invasive component is from the basement membrane.[11] However, relative to head and neck superficial invasive carcinomas, there are varying views as to which lesion does or does not qualify as microinvasive. Moreover, the pharynx has no lamina muscularis mucosae. Therefore,

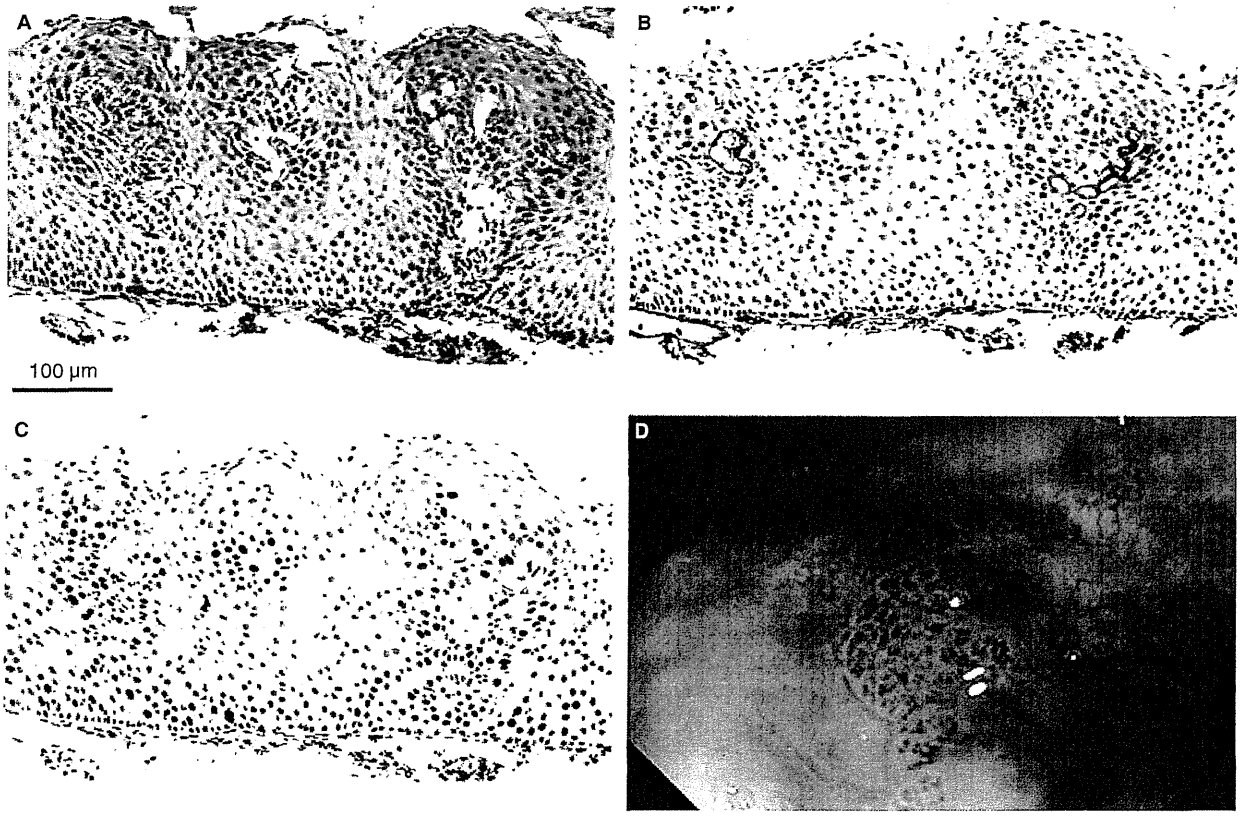

Figure 3. The histology of basal cell hyperplasia from a biopsy specimen. A, H&E. B, CD34. C, MIB-1. D, Narrow-band imaging of the oropharynx (posterior wall).

in the current study, only those cases in which at least one solitary carcinoma cell nest was observed in the subepithelial region were designated as invasive SCC of the pharynx. Usually, more than a solitary carcinoma cell nest was recognized but when a solitary carcinoma cell nest was recognized, it had to be distinguished from the involvement of minor salivary glands.

The thickness of IESCC was measured from the surface to the bottom of the thickest portion of IESCC. In order to minimize overestimation of epithelial thickness caused by tangential sectioning, resected specimens by EMR or ESD were unfolded on a plastic plate and fixed in 10% formalin overnight. The whole tissue specimen was then cut vertically and parallel at a thickness of <2 mm before embedding in paraffin. Then sections at a thickness of 2 μm were made and routinely evaluated. The epithelial thickness of whole area was measured in each case and the area of tissue without diathermy artefact was measured to register the thickness of IESCC.

To evaluate the depth of invasion in pharyngeal invasive SCC, the distance measured from the surface of the intraepithelial carcinoma to the bottom of the deepest portion of the invasive carcinoma tissue was regarded as tumour thickness.

MEASUREMENT OF MVD

The most densely vascularized area in the intraepithelial lesion that had the highest number of microvessels stained immunohistochemically by CD34 monoclonal antibody was selected as the hot spot. The area was photographed at a magnification of ×100. The intraepithelial microvascular area and carcinoma cell area were quantitatively determined on the image using ImageJ software (National Institute of Health, Bethesda, MD, USA). The percentage of microvascular area to tumour cell area was calculated and defined as MVD.

STATISTICAL ANALYSIS

Continuous variables, evaluated and recorded in detail, included means, medians, SDs, and maximum and minimum values. The mean values of variables with a normal distribution were compared with Student's

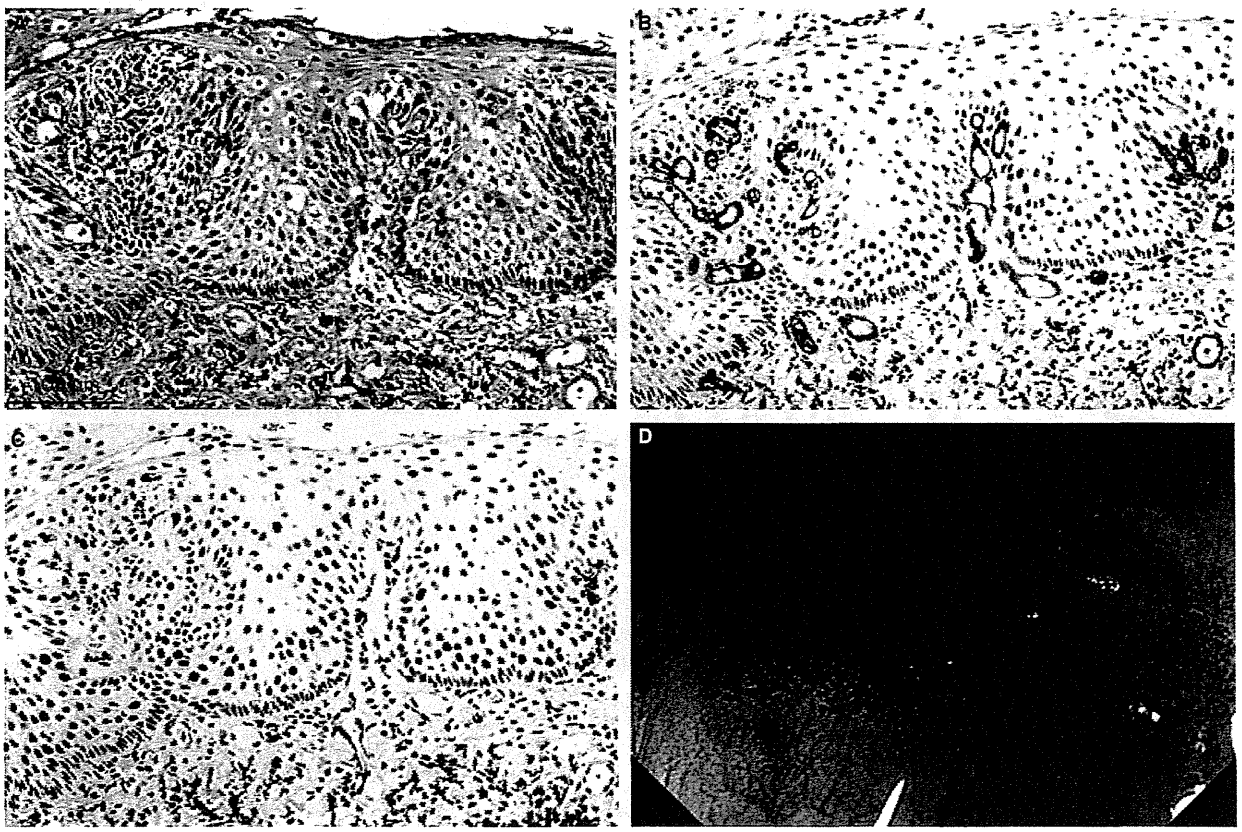

Figure 4. The histology of mild dysplasia from a biopsy specimen. A, H&E. B, CD34. C, MIB-1. D, Narrow-band imaging of the oropharynx (posterior wall).

t-test. When a normal distribution was not evident, the non-parametric Wilcoxon rank sum test was employed. Student's *t*-test was used to compare the thickness of an intraepithelial carcinoma in each categorized group according to parameters such as MVD. The associations of histological parameters with subepithelial invasion were assessed with χ^2 statistics. Spearman's rank correlation tests were employed to assess the relationship between MVD and the thickness of IESCC or the relationship between tumour thickness and tumour size. Values of $P < 0.05$ were considered significant.

Results

HISTOLOGICAL FINDINGS OF NON-NEOPLASTIC LESIONS, DYSPLASIA, SCC *IN SITU* AND INVASIVE SCC ON THE BASIS OF MICROVASCULAR IRREGULARITIES AND THE MATCHED NBI IMAGES

We highlighted several differential diagnostic findings such as IPCL extension upward, IPCL dilation and branching, IPCL diameter expansion, proliferative cell distribution, basal cell palisading, basal cell enlargement, spinous layer retention, superficial layer (parakeratotic-like flat epithelial cell layer) retention, nuclear arrangement, nuclear density and subepithelial solitary cell nest, as shown in Table 3. The microscopic images including H&E staining (A), immunohistochemical staining using CD34 (B) or MIB-1 (C) antibodies are shown in Figures 1–7. The matched NBI images (D), except for Figure 1, are also shown. In Figure 1, as a non-neoplastic and non-inflammatory squamous epithelium, an IPCL was observed and uniform basal cells were arranged in the basal layer, but no microvascular irregularities were observed. In Figure 2, biopsy specimen histology showed an inflammatory lesion. Intercellular oedema and intraepithelial inflammatory cells were recognizable. An upward shift of an almost normal-sized IPCL, but no IPCL irregularity was seen (Figure 2A–C). NBI endoscopy shows inflammatory lesions as an ill-demarcated brownish area. Slight IPCL proliferation and IPCL dilation are obscured by the

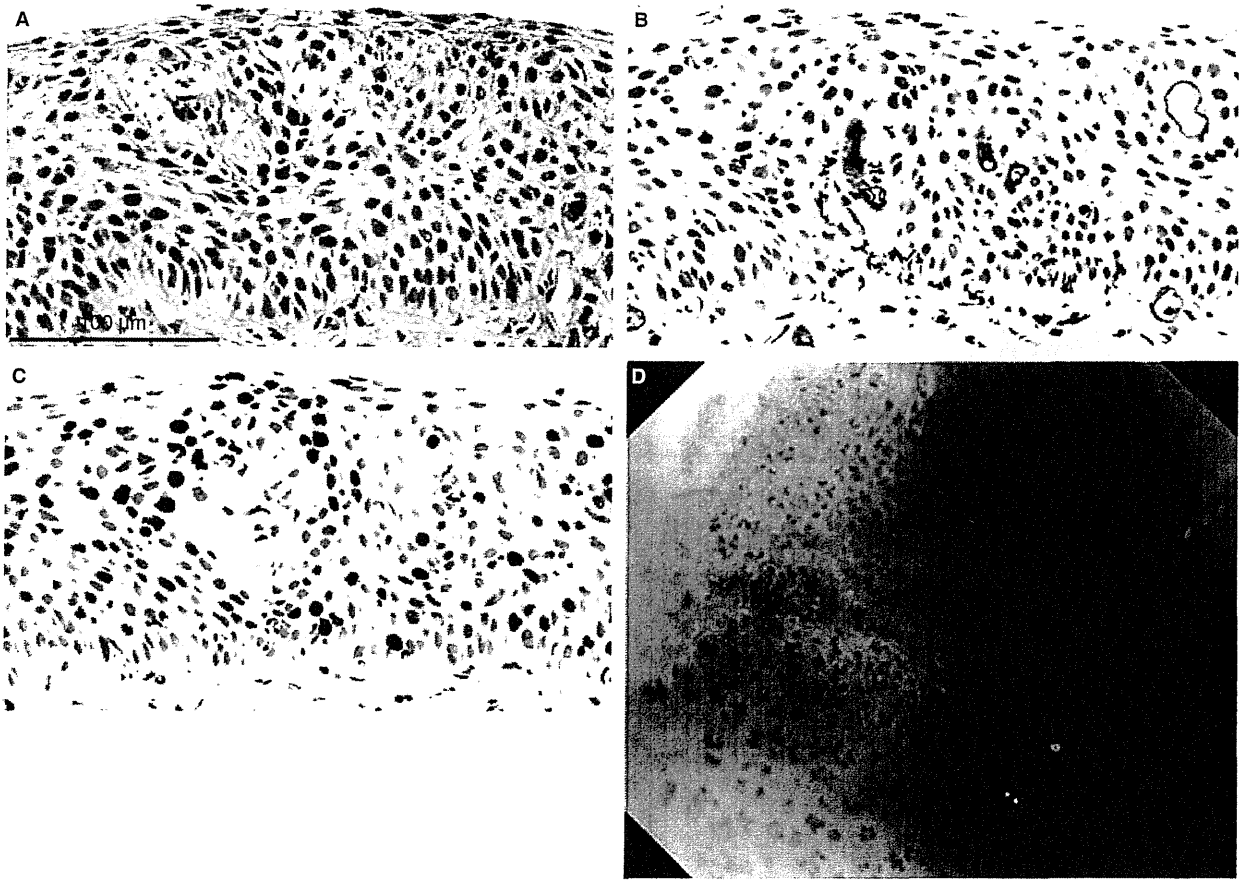

Figure 5. The histology of severe dysplasia from a biopsy specimen. A, H&E. B, CD34. C, MIB-1. D, Narrow-band imaging of the hypopharynx (pyriform sinus).

cloudy background mucosa (Figure 2D). Basal cell hyperplasia is shown in Figure 3. Proliferative cells labelled by MIB-1 were localized at the peri-IPCL. Basal cell palisading was preserved and no basal cell enlargement was detected. Spinous and surface layers were also preserved (Figure 3A–C). Figure 3 is presumed be an earlier manifestation of dysplasia, since thickened IPCLs with dilation and branching have shifted to the superficial side of the epithelium (Figure 3A). In contrast to inflammatory lesions, hyperplastic lesions showed small, well-demarcated brownish areas on NBI images with magnification (Figure 3D). Figure 4 shows mild dysplasia. Basal cell palisading was observed, though proliferative cells with enlarged nuclei, proliferating in a lamellar pattern, were limited to the lower third of the epithelial layer (Figure 4A–C). IPCL abnormalities such as IPCL extension upward, IPCL dilation and branching and IPCL diameter expansion were also recognized clearly, as well as basal cell hyperplasia (Figure 4A). The NBI image showed a wider brownish area than Figure 3D. In severe dysplasia (Figure 5), nuclear arrangement polarity was lost and nuclear density was severely increased throughout the intraepithelial layer, although there was maturation of the superficial portion of the epithelium. Microvascular irregularities were more severe than those in mild dysplasia. In the NBI image, dense, irregular IPCLs were recognized as a thicker and whitish epithelial lesion against a well-demarcated brownish area (Figure 5D). In SCC *in situ* (Figure 6), the basal cell palisading was obscure and the superficial maturation of the epithelium was lost. Prominent architectural disarray, marked cytological atypia and increased mitotic figures with pathological forms were recognized. Thickening of the intraepithelial

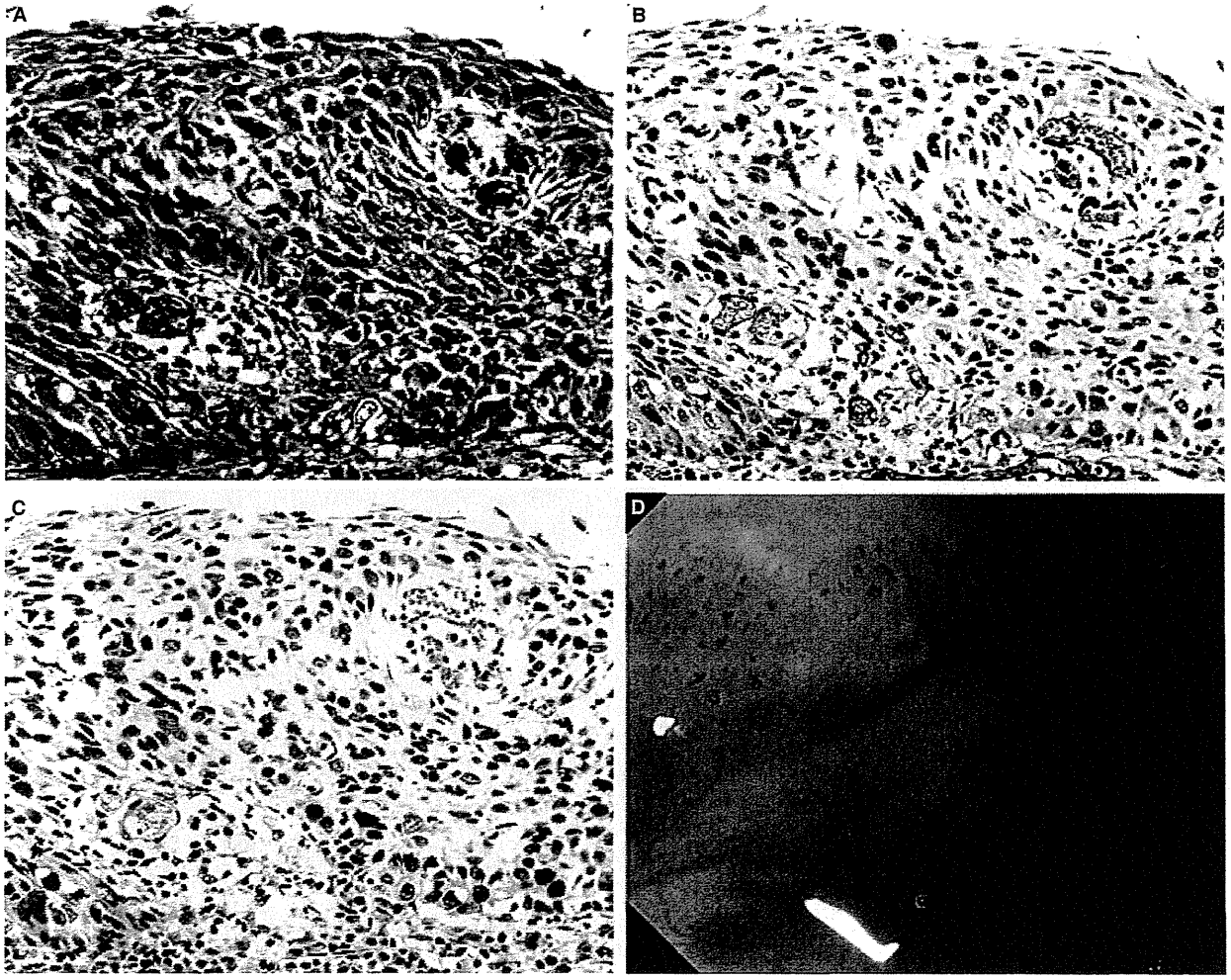

Figure 6. The histology of squamous cell carcinoma *in situ* from an endoscopically resected specimen. A, H&E. B, CD34. C, MIB-1. D, Narrow-band imaging of the hypopharynx (pyriform sinus).

lesion was also recognized as being different from that in severe dysplasia. IPCL dilation and IPCL branching-like petals were clearly recognized. The NBI image (Figure 6D) showed more dilated irregular IPCLs than Figures 4D and 5D. In invasive SCC (Figure 7), IESCC thickening and subepithelial solitary cell nests were recognized (Figure 7A–C). Dilated and branched IPCLs were recognized in the upper area of IESCC accompanied by thickening of IESCC. The NBI image showed a more voluminous and thickened brownish area (Figure 7D).

SUBEPITHELIAL INVASION, IESCC THICKNESSES AND TUMOUR THICKNESS OF INVASIVE SCC

The range of thickness of IESCC was broad: 125–1000 μm. The tumour thickness of invasive SCCs ranged from 300 to 3500 μm. The tumour thickness of all STPSCCs ranged from 125 to 3500 μm.

MVD

To calculate the MVD, immunohistochemistry using CD34 antibody was performed to detect microvessels clearly (Figures 1–7B). The values of MVD ranged from 0.1 to 17.82 (mean ± SD 4.04 ± 3.23).

RELATIONSHIPS BETWEEN HISTOLOGICAL PARAMETERS

There was a significant correlation between MVD and IESCC thickness ($P = 0.0115$, Spearman correlation test $r = 0.25$, Figure 8A). Interestingly, there was

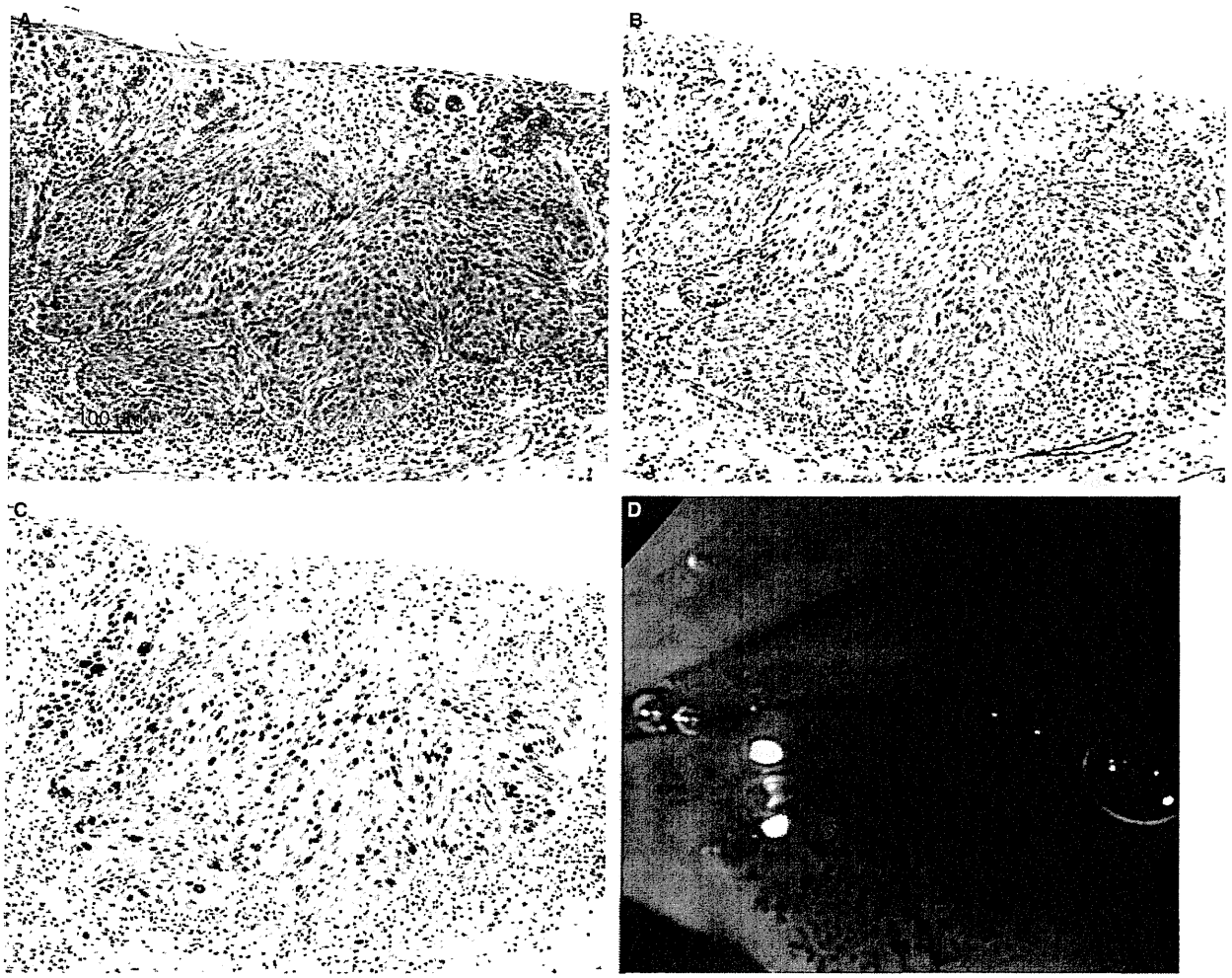

Figure 7. The histology of invasive squamous cell carcinoma from an endoscopically resected specimen. **A**, H&E. **B**, CD34. **C**, MIB-1. **D**, Narrow-band imaging of the oropharynx (lateral wall).

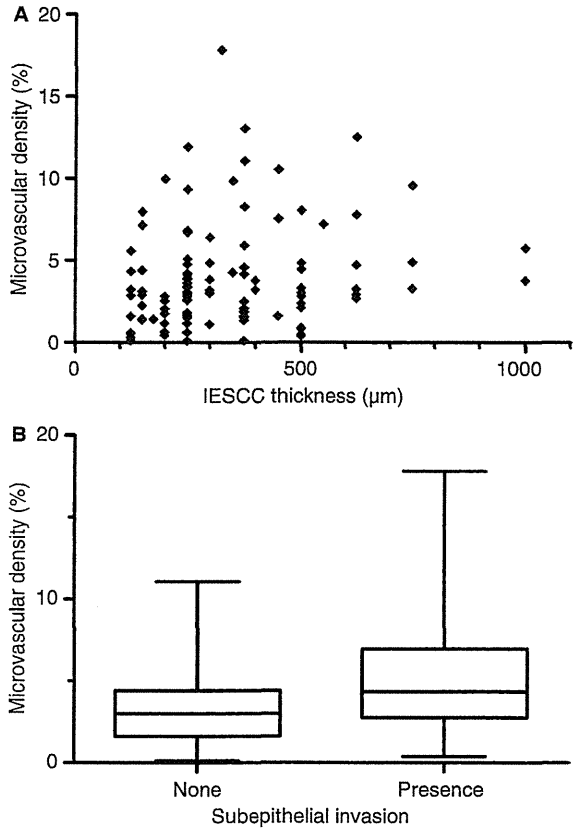

Figure 8. The relationships between intraepithelial squamous cell carcinoma (IESCC) thickness, microvascular density (MVD), and subepithelial invasion. **A**, The relationship between MVD and IESCC thickness. **B**, The relationship between MVD and subepithelial invasion. A *P*-value < 0.05 was taken to indicate a statistically significant difference.

significant correlation between MVD and subepithelial invasion ($P = 0.0078$, Figure 8B).

Next, we investigated the relationships between IESCC thickness, tumour thickness, tumour size and subepithelial invasion. There was significant correlation between IESCC thickness and subepithelial invasion ($P < 0.0001$, Figure 9A). There was significant correlation between tumour thickness and subepithelial invasion ($P < 0.0001$, Figure 9B). These correlations suggested that SCC detected by NBI endoscopy shows increased MVD due to microvascular irregularities, which then leads to greater IESCC thickness, resulting in subepithelial invasion.

The cases with subepithelial invasion had significantly larger tumours than those without subepithelial invasion ($P = 0.0013$, Figure 9C). There was significant correlation between tumour thickness and tumour size (Spearman $r = 0.4560$, $P < 0.0001$, Figure 9D).

As described above, there were significant correlations between tumour thickness, MVD and subepithelial invasion. We investigated the relationship between tumour thickness and vessel infiltration, including invasive and non-invasive carcinomas. As shown in Figure 9E, there was significant correlation between tumour thickness and vessel infiltration ($P < 0.0001$). Only one STPSCC (0.96%) showed lymph node metastasis as a late event (Table 2). The tumour thickness in this case was 1750 μm and both lymphatic and blood vessel infiltration were observed in the primary tumour. The mean tumour thickness of STPSCCs resected by EMR/ESD was 1040 μm. Three cases (2.9%) showed local recurrence after EMR/ESD. All three tumours were <20 mm in diameter but showed subepithelial invasion, and one of the three had blood vessel infiltration. The horizontal cut ends of specimens by EMR/ESD were positive for carcinoma cells.

Discussion

The dense microvascular proliferation caused by irregular branching of IPCLs, the upward shift and thickening of IPCLs, which reflect microvascular irregularities detected by NBI endoscopy, were observed pathologically in squamous epithelial lesions of the pharynx. The alterations of microvascular structures represented by IPCL irregularities occurred with architectural or cytological abnormalities in squamous epithelial lesions (Table 3). Based on the current results, we propose four steps to invasive SCC starting with basal cell hyperplasia. In the first step, the upward shift of IPCLs with dilation and branching occurs in basal cell hyperplasia (Figure 3). In the second step, density of IPCL increases in mild dysplasia (Figure 4). In the third step, microvascular irregularities increase with branching of IPCLs (Figure 5). Moreover, marked IPCL proliferation with irregular branching is observed throughout the intraepithelial layer. Thickening of intraepithelial lesions becomes apparent (Figure 6). Finally, in the fourth step, dilated and branched IPCL increases in intraepithelial lesions, accompanied by increasing MVD, resulting in subepithelial invasion (Figure 7).

The results of the present study suggest that IESCC thickening by increased MVD plays an important role in the early stage of subepithelial invasion (Figures 8 and 9). On the other hand, the average value of MVD of dysplasia (including mild and severe) was 2.9, which was lower than the average value of MVD of IESCC (4.0). The value of MVD of single basal cell hyperplasia was 2.1. This suggests that MVD increases step by step from basal cell hyperplasia through dysplasia to

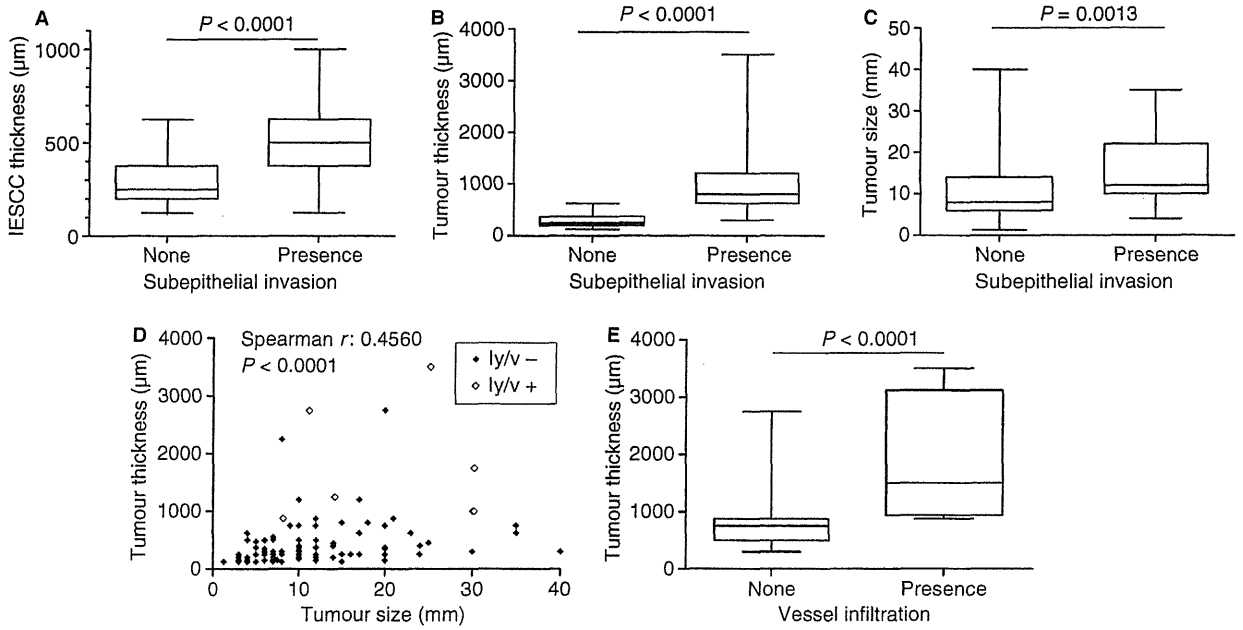

Figure 9. The relationships between intraepithelial squamous cell carcinoma (IESCC) thickness, tumour thickness, tumour size, subepithelial invasion, and vessel infiltration. A, The relationship between IESCC thickness and subepithelial invasion. B, The relationship between tumour thickness and subepithelial invasion. C, The relationship between tumour size and subepithelial invasion. D, The relationship between tumour thickness and tumour size. Black and white diamond symbols represent a case without lymphatic and venous infiltration and a case with lymphatic or venous infiltration, respectively. E, The relationship between tumour thickness and vessel infiltration in superficial-type pharyngeal squamous cell carcinomas (STPSCCs) with subepithelial invasion (n = 29). A P-value <0.05 was taken to indicate a statistically significant difference.

carcinoma. An interesting previous report examined MVD in epithelial proliferative lesions of breast.[12] In florid ductal hyperplasia usual type, atypical ductal hyperplasia and atypical lobular hyperplasia, MVD values were intermediate between normal glandular structures and neoplastic lesions. Moreover, the MVD of higher-grade-type intraductal carcinoma was higher than that of lower-grade-type intraductal carcinoma. These findings suggest that an increase in blood supply is necessary for any type of epithelial proliferation, and higher MVD values are associated with a higher risk of progression to invasiveness in pre-invasive breast cancer as in intraepithelial squamous lesions in the present study. However, because the number of precursor lesions in the present study was small, further detailed analysis is needed in the future.

There were a few tumours showing remarkable intraepithelial spreading without either subepithelial invasion of the STPSCC or thickening of IESCC. The five tumours without subepithelial invasion were > 20 mm (20 mm <), and these tumours were categorized as T2 in the International Union Against Cancer classification.[13] The cases were assumed to be good candidates for endoscopic resection of STPSCC. As shown in Figure 9E, there was significant correlation between tumour thickness and vessel infiltration in STPSCC. However, as shown in Figure 9E, the greater the tumour thickness, the higher rate of vessel infiltration that was observed. These results suggest that the T factor incorporating tumour thickness may be reasonable, as well as being a qualified risk factor, for clinicians when contemplating additional treatments such as lymph node dissection or selecting intense follow-up after EMR/ESD.

Multiple STPSCCs at oropharyngeal and hypopharyngeal mucosal sites were identified in 30 patients (43.5%) in the current study. This means that the same patient would need additional EMR/ESD. Numerous EMR/ESD can cause future stenosis of the pharynx. From the view of a preventive strategy, it is important to identify the abnormal proliferative factor influencing IPCL in STPSCC, and further future analyses are necessary.

The chance of diagnosing an early squamous epithelial lesion with microvascular irregularities detected by NBI endoscopy has improved and facilitates an understanding of the pathological features necessary for appropriate diagnosis. The present study has

shown microvascular irregularities to be associated with carcinogenesis of SCC. A better understanding of the pathogenesis of squamous epithelial lesions and early invasion of SCC should facilitate appropriate diagnosis and treatment of STPSCC.

Acknowledgements

We thank Ms Mai Okumoto for her excellent technical assistance in immunohistochemistry. This study was supported in part by a Grant-in-Aid for Cancer Research (19-10) from the Ministry of Health, Labour, and Welfare of Japan and a Grant-in-Aid for the Third Term Comprehensive 10-year Strategy for Cancer Control from the Ministry of Health, Labour, and Welfare of Japan.

References

1. Parkin DM, Pisani P, Ferlay J. Estimates of the worldwide incidence of 25 major cancers in 1990. *Int. J. Cancer* 1999; **80**; 827–841.
2. Nonaka S, Saito Y. Endoscopic diagnosis of pharyngeal carcinoma by NBI. *Endoscopy* 2008; **40**; 347–351.
3. Gono T, Yamazaki K, Doguchi N *et al.* Endoscopic observation of tissue by narrow band illumination. *Opt. Rev.* 2003; **10**; 211–215.
4. Inoue H, Honda T, Nagai K *et al.* Ultra-high maginification endoscopic observation of carcinoma *in situ* of the oesophagus. *Dig. Endosc.* 1997; **9**; 16–18.
5. Kumagai Y, Inoue H, Nagai K *et al.* Magnifying endoscopy, stereoscopic microscopy, and the microvascular architecture of superficial esophageal carcinoma. *Endoscopy* 2002; **34**; 369–375.
6. Barnes L, Eveson JW, Reichart P *et al.* eds. *Pathology and genetics of head and neck tumours: the World Health Organization classification of tumors*. Lyons: International Agency for Research on Cancer (IARC) Press, 2005.
7. Kodama M, Kakegawa T. Treatment of superficial cancer of the esophagus: a summary of responses to a questionnaire on superficial cancer of the esophagus in Japan. *Surgery* 1998; **123**; 432–439.
8. Asakage T, Yokose T, Mukai K *et al.* Tumor thickness predicts cervical metastasis in patients with stage I/II carcinoma of the tongue. *Cancer* 1998; **82**; 1443–1448.
9. Lim SC, Zhang S, Ishii G *et al.* Predictive markers for late cervical metastasis in stage I and II invasive squamous cell carcinoma of the oral tongue. *Clin. Cancer Res.* 2004; **10**; 166–172.
10. Muto M, Nakane M, Katada C *et al.* Squamous cell carcinoma *in situ* at oropharyngeal and hypopharyngeal mucosal sites. *Cancer* 2004; **101**; 1375–1381.
11. Barnes L. *Surgical pathology of the head and neck*, 2nd edn. New York, Basel: Informa Healthcare, Marcel Dekker, 2001.
12. Viacava P, Naccarato AG, Bocci G *et al.* Angiogenesis and VEGF expression in pre-invasive lesions of the human breast. *J. Pathol.* 2004; **204**; 140–146.
13. Sobin LH, Wittekind C eds. *International Union against Cancer TNM classification of malignant tumours*, 6th edn. New York: Wiley-Liss, 2002.

2010年5月10日発行

Nikkei Medical 日経メディカル

2010 5

特別編集版

消化管診療のトピックス＆トレンド

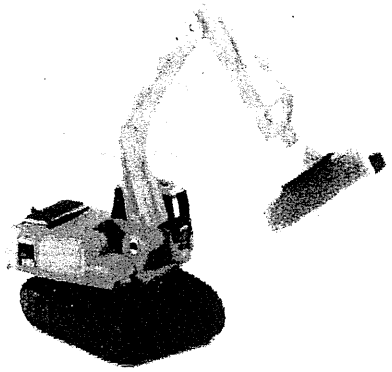

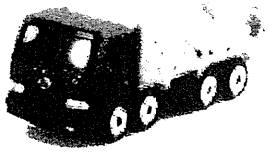

インタビュー
第6回日本消化管学会総会学術集会会長
飯田 三雄氏
「消化管学のさらなる発展に寄与したい」

特集 炎症性腸疾患を鎮める あの手この手

レポート
IBSの発症原因に新仮説が続々

診療アップデート
「小腸の内視鏡診断と治療」ほか

学会トピックスWIDE
胃シンチでFDの運動機能を評価

日本消化管学会監修

消化器アップデート UPDATE

咽頭・食道癌の最新知見

アルコールの発癌性にWHOが警鐘

アルコール飲料に含まれるエタノールが代謝される過程で産生されるアセトアルデヒドが、WHOでClassIの発癌物質として認定された。日本人の約半数はアセトアルデヒドの代謝酵素が低活性型もしくは不活性型であるため、飲酒による発癌リスクが高いと考えられている。

消化管疾患の知識

武藤 学（京都大学医学部消化器内科准教授）

2009年10月に世界保健機関（WHO）の下部組織である国際がん研究機関（International Agency for Research on Cancer:IARC）の会合が行われ、この会で初めて、アルコール飲料が代謝される際に発生するアセトアルデヒドが食道・頭頸部癌のClass Ⅰの発癌物質、つまり最も明らかな癌の原因物質であることが認定された。筆者もこの会議に参加し、2週間以上かけて様々な発癌物質を再評価する場に立ち会った。ヒトの体内で代謝によって産生される物質が発癌物質と認定されたのはこれが初めてのことだ。

食道癌と頭頸部の扁平上皮癌は多発または重複しやすく、このことは半世紀以上前から“フィールド癌化説（field cancerrization）”という理論で知られていた。アセトアルデヒドが食道・頭頸部の共通した発癌物質であることは、この現象からも説明がつく。

本稿では、近年、明らかになってきた、アルコールによる食道咽頭癌発生のメカニズムや、多発・重複癌が発生しやすい理由を紹介したい。

ALDH2の低活性型と不活性型はハイリスク

図1はアルコールの代謝過程だ。摂取されたアルコール飲料（エタノール）は、主に肝臓のミトコンドリアでアルコール脱水素酵素（ADH）によってアセトアルデヒドに代謝される。さらに、アセトアルデヒドは、アルデヒド脱水素酵素（ALDH）によって酢酸に代謝される。

アセトアルデヒドの代謝では、ALDHの一種のALDH2という酵素がアセトアルデヒドを主に除去する役割を担っている。そのため、飲酒後のアセトアルデヒドの血中濃度は、ALDH2活性型の人に比べ、ALDH2不活性型ヘテロの遺伝子型の酵素をもつ人（低活性型）は約6倍、ALDH2不活性型ホモの遺伝子型の酵素をもつ人（不活性型）は約19倍にも上昇する（表1）。

日本人の約半数は、ALDH2低活性型、もしくはALDH2不活性型である。これらの遺伝子型を持ってい

図1●アルコールの代謝過程

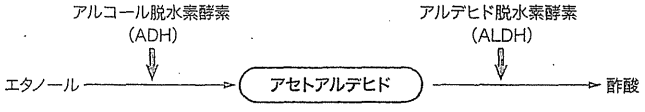

表1●飲酒後のアセトアルデヒドの相対血中濃度（武藤氏による）

ALDH2-活性型/活性型	1
ALDH2-活性型/不活性型	6
ALDH2-不活性型/不活性型	19

図2●食道・のどの癌化のメカニズム（武藤氏による）

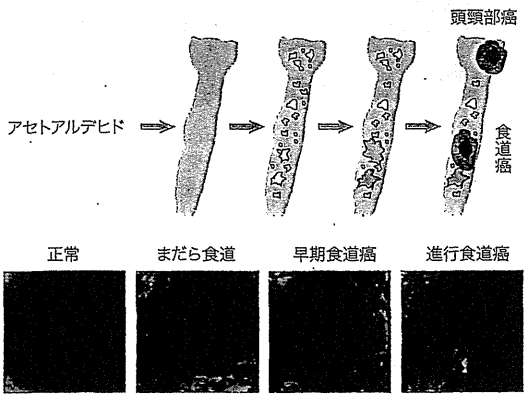

表2●頭頸部癌/食道癌症例におけるまだら食道（multiple LVL）発生予測因子

因子	相対危険度（95% CI）	p
ALDH2不活性型遺伝子を持つ人（大半が低活性型）	5.8（2.9-11.6）	<0.0001
低活性ADH3遺伝子	2.8（1.1-6.7）	0.019
男性	2.3（0.5-12.2）	0.32
60歳以上	1.5（0.8-2.8）	0.27
たばこ指数（1日本数×年数）≧1000	1.0（0.5-1.8）	0.88
1日摂取アルコール量≧80g	0.9（0.5-1.8）	0.84

M Muto, et al. Carcinogenesis 2005 ;26 ;1008-12.

る人は、飲酒により顔面紅潮や動悸を起こすので、この反応によって9割以上の人のALDH2遺伝子型を大まかに判別することができる。ALDH2不活性型の人は極端にお酒に弱いため、お酒は全く飲めない。しかし、ALDH2低活性型の人は飲酒を繰り返すうちにある程度お酒が飲めるようになる。こうした人がアルコール飲料を飲むと食道癌になりやすいことが実際の報告からも明らかになっている。

ALDH2活性型の人の場合でも、1日1合の日本酒換算量を飲む場合を基準とすると、2合飲むと食道癌のリスクは5倍、3合飲むと10倍のリスクになる。一方、ALDH2低活性型の人が1日1合の日本酒換算量を飲む場合は、ALDH2活性型の人が1日1合の日本酒換算量を飲む場合に比べて、食道癌のリスクは5倍、2合飲むと食道癌のリスクは実に50倍以上、3合飲むと80倍にもなる（Yokoyama A, Muto M, et al. Carcinogenesis 2002;23:1851-9）。

“まだら食道”が食道癌に進展

内視鏡検査を行うと、ヨード染色にて大小不同のヨード不染帯を多発するいわゆる“まだら食道”を来す患者に遭遇することがある。このまだら食道は、放置すると上皮内腫瘍が出現し、扁平上皮癌へと移行し、2～3年もすれば進行癌になる（図2）。

我々の調査で、このまだら食道はALDH2不活性型遺伝子を持つ人で出現しやすいことが明らかになった（表2）。頭頸部癌もしくは食道癌の患者におけるまだら食道の発生予測因子を調べたところ、ALDH2活性型の人に比べて、ALDH2不活性型とALDH2低活性型の人の相対危険度は5.8と、年齢や喫煙より高いことが分かった。ALDH2不活性型遺伝子を持つ人のほとんどは、ALDH2低活性型だった。病変が広範にわたるまだら食道から発癌すると、冒頭のように頭頸部や食道に多発・重複癌が発生するというわけだ。

写真1●全身麻酔下内視鏡的咽頭粘膜切除術（提供：武藤氏）

図3●食道癌EMR例におけるヨード不染帯の程度別の食道内多発癌発生頻度

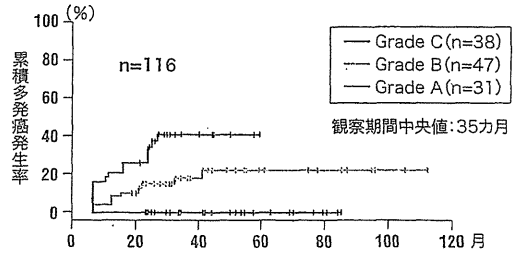

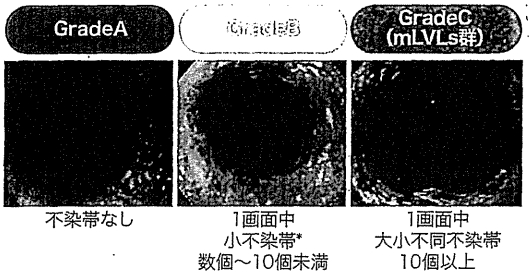

*小不染帯とは5mm以下のヨード不染帯を示す

堅田親利、武藤学ほか. 胃と腸 2007;42(9):1355-63.

頭頸部癌の早期発見が可能になった

多発・重複癌発生メカニズムが明らかになったことに加え、Narrow Band Imaging (NBI)や拡大内視鏡といった内視鏡技術の進歩により、これまで極めて困難といわれていた頭頸部、特に咽頭・喉頭の扁平上皮癌の早期発見が可能になった。早期発見した咽頭・喉頭の表在癌に対しては、低侵襲である全身麻酔下での内視鏡的切除が行われるようになった。

我々は、川崎市立病院耳鼻咽喉科の佐藤靖夫氏らが開発した湾曲型喉頭鏡を用いて、全身麻酔下の内視鏡的切除術を行っている（写真1）。通常、内視鏡で見ると左右の梨状陥凹はつぶれているが、湾曲型喉頭鏡を用いると喉頭が持ち上がり、食道入口部まで見える。視野が確保されやすくなり、非常に内視鏡切除術が行いやすい。

4分の3周以上の病変は7割が再狭窄

まだら食道から移行した食道癌は、病変が広範囲に及ぶため、治療に難渋することが多い。食道癌の治療は、内視鏡的治療や外科的切除、抗癌剤治療、放射線など、ステージ別に様々な選択肢がある。中でも内視鏡的粘膜切除術（Endoscopic mucosal resection:EMR）や粘膜下層剥離術（Endoscopic submucosal dissection:ESD）は、低侵襲で根治性のある治療法として広く行われているが、周在性が大きい病変や全周性の病変では、治療後の食道狭窄を来すため適応にならない。

EMR後の粘膜欠損の周在性と食道狭窄の頻度を調べると、粘膜欠損が4分の3までの場合は、食道の再狭窄を来した患者はいなかったが、4分の3周以上の病変を取った場合には狭窄率は一気に跳ね上がり、約7割の人で狭窄が起きていた。3cm以上の長い病変になると狭窄はほぼ100％近い値になる。

ヨード不染帯の程度によって再発率に大きな違い

食道癌の外科手術例における10年以内の2次癌の発生リスクを部位別にみると、胃癌の相対危険度が2.0、肺癌が3.24であるのに対し、頭頸部癌は実に34.9と突出して多くなっている。まだら食道から移行した食道癌は、内視鏡により病変を取り除いても、その後、異時性の癌が発生する可能性が高い。

EMR後の食道癌における異時性の食道内多発癌の発生率は、ヨード不染帯の数が多くなるに従って高くなる（図3）。筆者は、GradeBやGradeCの患者には半年から1年に1回程度の検査が必要と考える。また、逆に、不染帯がない患者は3年に1回程度の検査でよい可能性がある。

エタノールの代謝産物のアセトアルデヒドには発癌性があり食道癌を来しやすい。アセトアルデヒドによる食道癌は、多発性の病変や重複頭頸部癌を伴うため、治療方針に難渋したり、再発率が高いといった課題が残る。そのため、飲酒により顔面紅潮などを起こすALDH2低活性型・不活性型と考えられる人は、過剰なアルコール摂取を控えることが重要である。

World Journal of Gastroenterology

Online Submissions: http://www.wjgnet.com/1007-9327office
wjg@wjgnet.com
doi:10.3748/wjg.v16.i23.2907

World J Gastroenterol 2010 June 21; 16(23): 2907-2912
ISSN 1007-9327 (print)

BRIEF ARTICLE

Endoscopic diagnosis of cytomegalovirus gastritis after allogeneic hematopoietic stem cell transplantation

Yasuo Kakugawa, Masahiro Kami, Takahisa Matsuda, Yutaka Saito, Sung-Won Kim, Takahiro Fukuda, Shin-ichiro Mori, Tadakazu Shimoda, Ryuji Tanosaki, Daizo Saito

Yasuo Kakugawa, Takahisa Matsuda, Yutaka Saito, Daizo Saito, Division of Endoscopy, National Cancer Center Hospital, Tokyo 104-0045, Japan
Masahiro Kami, Division of Exploratory Research, Institute of Medical Science, University of Tokyo, Tokyo 108-0071, Japan
Sung-Won Kim, Takahiro Fukuda, Shin-ichiro Mori, Ryuji Tanosaki, Division of Hematopoietic Stem Cell Transplantation, National Cancer Center Hospital, Tokyo 104-0045, Japan
Tadakazu Shimoda, Clinical Laboratory Division, National Cancer Center Hospital, Tokyo 104-0045, Japan
Author contributions: Kakugawa Y participated in the design of the study, data acquisition and interpretation, performed endoscopic examinations, and wrote the first draft of the manuscript; Kami M managed the therapy of patients, participated in the design of the study, and contributed to the writing of the manuscript; Matsuda T and Saito Y performed endoscopic examinations, and contributed to the writing of the manuscript; Kim SW, Fukuda T, Mori S and Tanosaki R managed the therapy of patients, and contributed to the writing of the manuscript; Shimoda T made the pathological diagnosis and contributed to the writing of the manuscript; Saito D participated in the design of the study and contributed to the writing of the manuscript; all authors read and approved the submitted version of the manuscript.
Correspondence to: Yasuo Kakugawa, MD, Division of Endoscopy, National Cancer Center Hospital, 5-1-1 Tsukiji, Chuo-ku, Tokyo 104-0045, Japan. yakakuga@ncc.go.jp
Telephone: +81-3-35422511 Fax: +81-3-35423815
Received: March 19, 2010 Revised: April 6, 2010
Accepted: April 13, 2010
Published online: June 21, 2010

Abstract

AIM: To clarify the endoscopic and clinical findings of cytomegalovirus (CMV) gastritis after allogeneic hematopoietic stem cell transplantation (allo-SCT).

METHODS: Between 1999 and 2005, 523 patients underwent allo-SCT at our hospital, and 115 of these patients with gastrointestinal symptoms underwent esophagogastroduodenoscopy.

RESULTS: CMV gastritis was diagnosed pathologically in seven patients (1.3%) with the other 108 patients serving as controls. Six of the seven patients developed positive CMV antigenemia, and five complained of abdominal pain. Development of abdominal pain preceded CMV antigenemia in four of the five patients. Endoscopic examination showed oozing (n = 2), erosion (n = 6), and redness (n = 5) in the seven patients with CMV gastritis, while the control patients showed oozing (n = 3), erosion (n = 24), and redness (n = 100). Erosion and oozing were more frequently documented in patients with CMV gastritis compared with the controls, and the differences were statistically significant (P = 0.0012 and 0.029, respectively). CMV inclusion bodies were documented in 12 of 14 biopsy specimens obtained from erosive lesions, while they were identified in 4 of 15 biopsy specimens obtained from lesions other than erosions (P = 0.0025).

CONCLUSION: This study suggests that erosion and oozing, as well as abdominal pain, are useful indicators in the diagnosis of CMV gastritis following allo-SCT.

Key words: Cytomegalovirus gastritis; Hematopoietic stem cell transplantation; Cytomegalovirus antigenemia; Esophagogastroduodenoscopy; Graft-versus-host disease

Peer reviewer: Dr. Herwig R Cerwenka, Professor, Department of Surgery, Medical University of Graz, Auenbruggerplatz 29, A-8036 Graz, Austria

Kakugawa Y, Kami M, Matsuda T, Saito Y, Kim SW, Fukuda T, Mori S, Shimoda T, Tanosaki R, Saito D. Endoscopic diagnosis of cytomegalovirus gastritis after allogeneic hematopoietic stem cell transplantation. *World J Gastroenterol* 2010; 16(23): 2907-2912 Available from: URL: http://www.wjgnet.com/1007-9327/full/v16/i23/2907.htm DOI: http://dx.doi.org/10.3748/wjg.v16.i23.2907

INTRODUCTION

Cytomegalovirus (CMV) disease is a serious complication after allogeneic hematopoietic stem cell transplantation (allo-SCT)[1], which is widely accepted as a curative therapy for advanced hematological malignancies including leukemia and malignant lymphoma. CMV disease can involve many organs and the gastrointestinal (GI) tract is a common target[2].

CMV antigenemia is one of the most widely used methods to detect CMV reactivation in a variety of clinical settings[3]; however, it is of limited value in predicting and diagnosing GI CMV disease[4]. GI CMV disease is usually diagnosed based on pathological examination of endoscopically obtained mucosal biopsy specimens. Few reports have been published regarding endoscopic examination in diagnosing CMV gastritis after allo-SCT[5-7]. This study aimed to investigate endoscopic findings of CMV gastritis after allo-SCT in addition to its clinical features.

MATERIALS AND METHODS

Study patients

Between January 1999 and September 2005, 523 patients underwent allo-SCT at the National Cancer Center Hospital in Tokyo, Japan. Among them, 115 patients with GI symptoms underwent esophagogastroduodenoscopy (EGD). Written informed consent was obtained from all patients before EGD. We retrospectively reviewed records of medical, endoscopic and pathological examination in the 115 EGD patients. CMV gastritis was diagnosed pathologically in seven patients (1.3%) by hematoxylin-eosin staining and immunohistochemical staining with an anti-CMV antibody. The other 108 patients served as controls.

Endoscopic procedure

All EGD patients orally received 100 mL of a solution containing 1 g of pronase and 1 g of sodium bicarbonate to remove mucus and bubbles on the gastric mucosa before EGD. Antiperistaltic agents (scopolamine butylbromide 20 mg or glucagon 1 mg) and sedatives (pethidine hydrochloride 17.5-35 mg or midazolam 2-3 mg) were injected intravenously. Conventional endoscopic instruments (GIF Q240; Olympus Co, Ltd, Tokyo, Japan) were used, and biopsy specimens were obtained endoscopically from severely involved areas. When abnormal findings were not found, biopsy specimens were obtained from normal appearing areas.

Pathological examination

Biopsy specimens were fixed immediately in a 10% buffered formalin solution and subsequently stained with hematoxylin-eosin. All tissues were examined by expert pathologists. Diagnosis of CMV gastritis was based on histological identification of CMV inclusion bodies by hematoxylin-eosin staining and immunohistochemical staining with an anti-CMV antibody. Diagnosis of graft-versus-host disease (GVHD) was determined in accordance with a report published previously[8].

Management of CMV

All patients were monitored at least once a week for CMV reactivation by CMV antigenemia assay using monoclonal antibody against C7-HRP (Teijin, Tokyo, Japan) after engraftment.

A patient was considered to be infected with CMV when CMV antigenemia assay detected CMV in the blood. A patient was considered to have CMV disease when CMV was demonstrated in biopsy specimens by hematoxylin-eosin staining and immunohistochemical analysis. Ganciclovir was initiated when either more than 10 cells per 50 000 cells were positive according to the CMV antigenemia assay in patients transplanted from related donors, a single cell per 50 000 cells was positive in patients transplanted from unrelated donors, or a patient was diagnosed as having CMV disease[9].

Management of GVHD

Acute GVHD was graded according to the consensus criteria[10,11] and all patients with grades II-IV acute GVHD were treated with 0.5-2.0 mg/kg per day of methylprednisolone.

Statistical analysis

Univariate analysis using Fisher's exact test was performed to compare differences in patient characteristics, clinical features, and endoscopic findings between the seven patients with CMV gastritis and the other 108 patients who had GI symptoms, but did not have CMV gastritis. Values of $P < 0.05$ were considered significant.

RESULTS

Patient characteristics

Patient characteristics are shown in Table 1. There was a significant difference in the number of patients given tacrolimus with methotrexate as GVHD prophylaxis between the two groups ($P = 0.018$).

Clinical features

Five of the seven patients with CMV gastritis complained of abdominal pain, while 31 of the 108 control patients complained of abdominal pain ($P = 0.030$) (Table 2). The pain was localized in the upper abdomen in all four patients with CMV gastritis whose medical reports provided the specific location of their pain (Table 3). Three patients required significant analgesia (morphine hydrochloride for one and pentazocine hydrochloride for the other two). Abdominal pain improved with ganciclovir in four of the five patients with abdominal pain, and the remaining patient (Case 1) died of bacterial pneumonia without any improvement in CMV gastritis.

Watery diarrhea was found in four of the seven patients with CMV gastritis, and was complicated by intes-

Table 1 Patient characteristics with and without CMV gastritis

Variables		Patients with CMV gastritis (n = 7)	Patients without CMV gastritis (n = 108)
Median age (range)		47 (26-62)	45 (18-69)
Gender	Male/female	5/2	65/43
Underlying diseases	Acute leukemia	1	41
	Chronic leukemia	2	15
	Malignant lymphoma	3	21
	Myelodysplastic syndrome	1	22
	Others	0	9
Preparative regimens	Myeloablative/reduced-intensity	2/5	48/60
Stem cell sources	Marrow/peripheral blood/cord blood	3/3/1	39/64/5
GVHD prophylaxis	CSP alone/CSP + MTX/CSP + MMF/FK506 + MTX/FK506 Alone	2/3/0/2[a]/0	36/64/2/2[a]/4

CMV: Cytomegalovirus; GVHD: Graft-versus host disease; CSP: Cyclosporine; MTX: Methotrexate; MMF: Mycophenolate mofetil; FK506: Tacrolimus. [a]P = 0.018.

Table 2 Clinical features in patients with and without CMV gastritis

Variables			Patients with CMV gastritis (n = 7)	Patients without CMV gastritis (n = 108)
Gastrointestinal symptoms at EGD		Nausea	2	60
		Vomiting	1	26
		Abdominal pain	5[a]	31[a]
		Abdominal discomfort	2	23
		Hematemesis	1	2
		Tarry stool	2	6
		Watery diarrhea	4	32
		Appetite loss	0	40
CMV	Median onset of CMV gastritis	Days (range)	63 (33-167)	NA
	CMV antigenemia (C7-HRP) at EGD	Positive/negative/not done	6[b]/1/0	28[b]/71/9
		Median number of positive cells per 50 000 (range)	8[d] (0-143)	0[d] (0-167)
	Involved organs of CMV diseases	Esophagitis/duodenitis/enterocolitis/pneumonitis/retinitis	1/2/1/0/0	0/0/4/0/0
GVHD		Positive (clinical grade: I / II / III / IV)	7[c] (2/2/3/0)	65[c] (45/10/9/1)

EGD: Esophagogastroduodenoscopy; NA: Not applicable. [a]P = 0.030, [b]P = 0.0026, [c]P = 0.044, [d]P = 0.0023.

Table 3 Clinical features of CMV gastritis

	Demographics	Gastrointestinal symptoms			CMV antigenemia assay	
	Age (yr), gender, diagnosis	Any symptoms	Abdominal pain		Onset (d)	Level at EGD (cells per 50000)
			Onset (d)	Localization in abdomen		
Case 1	34, male, CML	Abdominal pain, tarry stool	81	Upper abdomen	88	8
Case 2	43, female, MDS	Nausea, abdominal pain, tarry stool, hematemesis, watery diarrhea	53	No description	69	2
Case 3	60, male, AML	Abdominal pain, watery diarrhea	62	Upper abdomen	73	143
Case 4	48, female, ML	Abdominal pain, watery diarrhea	36	Upper abdomen	31	10
Case 5	47, male, ML	Abdominal pain, watery diarrhea	30	Upper abdomen	32	4
Case 6	62, male, CML	Abdominal discomfort	NA	NA	47	32
Case 7	26, male, ML	Nausea, vomiting, abdominal discomfort	NA	NA	NA	0[1]

[1]CMV antigenemia remained negative throughout clinical course. CML: Chronic myelocytic leukemia; MDS: Myelodysplastic syndrome; AML: Acute myelocytic leukemia; ML: Malignant lymphoma.

tinal GVHD in three of these four patients. Watery diarrhea improved with ganciclovir in a patient with CMV gastritis who had no evidence of intestinal GVHD.

All seven patients with CMV gastritis had GVHD, while 65 of the 108 control patients had GVHD (P = 0.044) (Table 2). Five of the seven patients with CMV gastritis had grade II-IV GVHD that was being treated by corticosteroids.

CMV antigenemia assay

Six of the seven patients with CMV gastritis and 28 of the 108 controls showed positive CMV antigenemia (P =